Proceedings of the 7th International Conference on HydroScience and Engineering

Philadelphia, USA September 10-13, 2006 (ICHE 2006)

ISBN: 0977447405

Drexel University

College of Engineering

PRELIMINARY HYDRODYNAMIC MODELING OF TIDAL CIRCULATION IN GLACIER BAY, ALASKA

Ralph T. Cheng[1] and S. James Taggart[2] and Julie K. Nielsen[2]

ABSTRACT

Glacier Bay is a recently (230 years ago) deglaciated fjord located within Glacier Bay National Park in southeastern Alaska. Glacier Bay is about 100 km long along the main axis, and it has several side arms and multiple sills, which are backed by very deep basins (200-400 m) with tidewater glaciers. Glacier Bay experiences a large amount of "runoff" from melting glaciers, high sedimentation, and large tidal ranges. The freshwater inflows from melting glaciers support estuarine circulation, possibly all year-round during recent warm winters. The complex topography and strong tidal currents lead to highly variable salinity, temperature, and current patterns within a small area. To characterize the hydrodynamics of this complex system, a 3D numerical hydrodynamic model (UnTRIM) using an unstructured grid has been implemented to simulate tidal circulation and salinity distribution in Glacier Bay, Alaska. The unstructured grid used by the model allows an accurate representation of the complex basin topography. Only very limited time-series records of water levels and current measurements had been taken. Some profiling ADCP and CTD cruises provided data for qualitative comparison with results of the numerical model. An open boundary exists at the southern end of the model near Gustavus where water levels (tides) and salinity values are specified. At tidewater glaciers, freshwater releases are assumed representing melting glaciers. Preliminary model simulations show complex spatial variations of tidal current pattern and salinity distributions are also computed. The model results are qualitative and preliminary, but they shed light on the overall hydrodynamic characteristics of Glacier Bay. These results are the basis for future interactive interdisciplinary research linking hydrodynamic processes to the distribution and abundance of marine animals in Glacier Bay National Park.

1. INTRODUCTION

Glacier Bay Alaska is a recently deglaciated fjord located within Glacier Bay National Park and Preserve in southeastern Alaska. The most recent deglaciation of Glacier Bay began approximately 230 years ago, when glaciers extended to the mouth of the bay. Glacial advance and retreat within Glacier Bay has created a complex network of fjords that continues to be highly influenced by glacial activity. The main channel splits into two major arms; the distance between the end of each arm and the entrance of the bay is approximately 100 km. Each arm has several side arms and multiple sills adjacent to very deep basins (200-400 m) and tidewater glaciers (Figure 1). Complex geometry in Glacier Bay results in complicated hydrodynamic and oceanographic processes. Parts of the bay can be characterized as fjords and other parts as estuaries or bays. A number of sills separate the bay into different oceanographic regimes. A large amount of freshwater "runoff" from melting glaciers enters into Glacier Bay, resulting in high sedimentation and low salinities. The

[1] Senior Research Hydrologist, U.S. Geological Survey, Menlo Park, CA 94025 (rtcheng@usgs.gov)
[2] Fisheries Research Scientist, U.S. Geological Survey, Alaska Science Center, Juneau, AK 99801 (jim_taggart@usgs.gov; Julie_nielsen@usgs.gov)

freshwater inflows from melting glaciers support vertical stratification and the formation of estuarine (gravitational) circulation. Freshwater input could occur year-round during warm winters. Melting glaciers create stratifications near the head of Glacier Bay that are similar to freshwater inflow in typical estuaries. Because of the great depth in the arms of Glacier Bay, the density stratification leads to strong gravitational circulation and possibly zones of turbidity maxima. The tidal range is about 7 m during Spring tides that drive tidal currents up to 2-3 m/sec near sills while the currents over deep channels are usually weak. The complex topography and strong tidal currents lead to highly variable salinity, temperature, and currents within a small area.

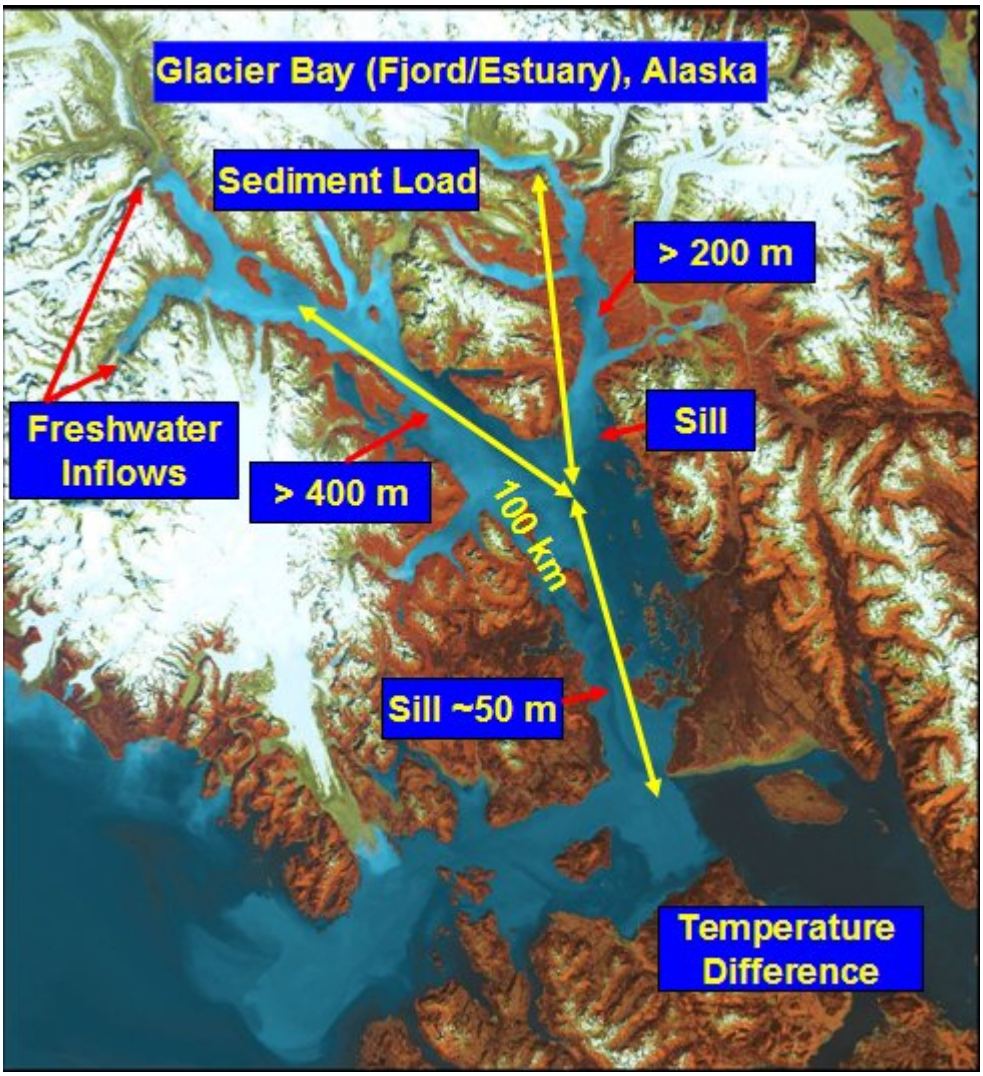

Figure 1. Complex geometry of Glacier Bay, Alaska

2. REVIEW OF AVAILABLE HYDRODYNAMIC DATA

Most of the existing field data consist of seasonal CTD sampling at a series of fixed stations occupied by the USGS, Figure 2; these results are reported by Hooge and Hooge (2002). These CTD data represent periodic snap shots of the physical oceanographic properties in the main channels of Glacier Bay, and the field data sampling efforts are continuing at the USGS. Interpretations of field data are assisted by AVHRR and Landsat TM imageries. These imageries are also discrete in time and often dependent upon the cloud coverage over the Bay. When a good image is available, it shows rather revealing oceanic processes, some of them will be discussed in section 3.1.

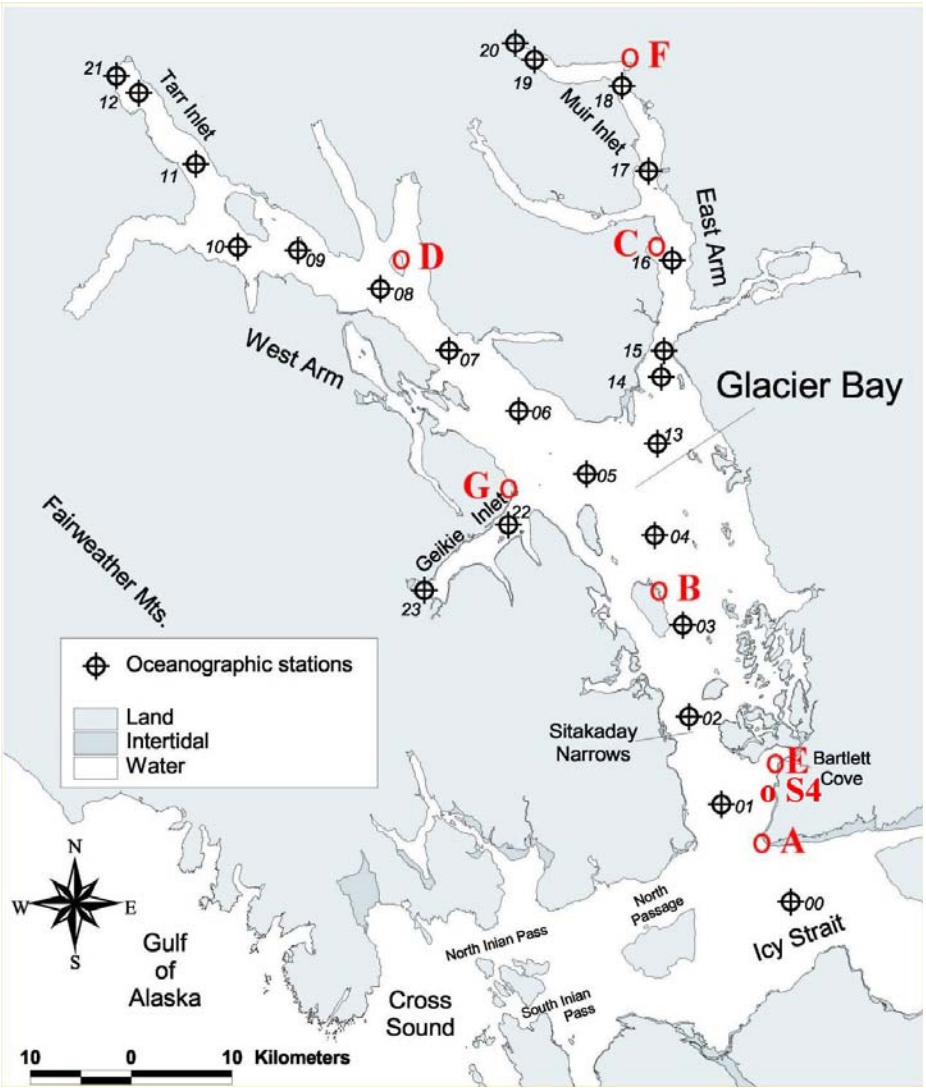

Figure 2. Locations of USGS fixed oceanographic stations (adapted from Hooge and Hooge, 2002). The red circles are locations where some tidal records are available. S4 is the location of the only known current meter deployment in 2001.

The National Oceanic and Atmospheric Administration (NOAA) collected a very limited set of time-series tide records at a few locations over the 100 km long system (see Figure 2 and Table 1). NOAA operated three historical tide stations in the 1950's and 1970's at Composite Island (D), Muir Inlet (C) and Willoughby Island (B), although these stations have since been removed. An hourly time-series record of water levels at Bartlett Cove (E) was collected for two and a half years between 1966 and 1968. More recent data are available at Point Gustavus (A) for less than 30 days in 1999. NOAA considers these data provisional; they are not officially entered into NOAA's tidal data database. These tidal records were digitized from the original hand-written or type-written data sheets for analysis. Harmonic analysis is a standard technique used to analyze tidal time-series. A least-squares harmonic analysis is applied to the time-series resulting in decomposing the time-series into a set of tidal constituents of well know frequencies whose amplitudes and phases are known as harmonic constants (Foreman, 1977). The harmonic constants are supposed to be stationary in time; if so, they can be used to predict tidal variations for any time period.

Table 1. Available Tides Data collected by NOAA in Glacier Bay, Alaska

NOAA	Start Date	End Date
Pt. Gustavus (A)	5/18/1999	6/8/1999
Willoughby Is. (B)	8/3/1959	10/2/1959
Muir Inlet (C)	7/27/1959	9/29/1959
Muir Inlet (C)	8/29/1972	9/27/1972
Composite Is. (D)	7/27/1959	9/28/1959
Bartlett Cove (E)	4/22/1966	7/31/1968

To ascertain that the harmonic constants are stationary, the time-series of tides at Bartlett Cove was analyzed in three segments: 1) April to December 1966; 2) January to December 1967; and 3) January to July 1968. These three time-series were analyzed independently, and the results of the analysis are given in Table 2. The differences in amplitude and phase of the major tidal constituents (M_2 and K_1) are less than 1 cm and 1 degree from the mean, respectively. Other major constituents have similar properties; the values for K_2 are slightly larger. More importantly, these results suggest that the harmonic constants derived for Bartlett Cove are stationary; thus they can be reliably used to predict tidal water levels for other periods of time. For the subsequent numerical modeling, the water level boundary conditions at the entrance of Glacier Bay will be generated by using this set of harmonic constants.

Table 2. Major harmonic constants deduced from the 1966, 1967, and 1968 Water level time-series at Bartlett Cove, Alaska

			1966	1967	1968	1966	1967	1968
Constituents	Amp	Phase		Amp			Phase	
O1	31.84	13.6	32.33	31.55	31.64	138.92	139.20	138.31
P1	16.52	9.31	17.12	16.34	16.11	143.73	144.44	143.65
K1	51.43	11.53	50.53	51.93	51.84	147.13	147.17	146.39
N2	36.01	140.17	35.45	36.23	36.35	34.83	37.54	36.02
M2	176.3	155.51	175.4	177.17	176.34	57.01	57.32	54.79
S2	58.23	172.13	56.55	58.91	59.22	80.80	83.31	82.28
K2	16.15	166.52	15.18	16.36	16.9	81.97	76.16	73.66

The other tidal data given in Table 1 were relatively short and taken at different times; these records were also harmonically analyzed, but a detailed quality assurance cannot be carried out because the time-series are not of sufficient length.

Measurements of tidal current are more scarce. On August 8, 2003, NOAA carried out a one-time cruise ADCP survey in Glacier Bay and reported spatial velocity distribution of the current velocity as shown in Figure 3 (Adapted with permission from Cokelet et al., 2006). Although this is a snapshot of velocity distribution, it is interesting to note that high velocity is concentrated near the entrance region of the bay, south of Sitakaday Narrows (sill), Figure 2, where velocities of up 200 - 300 cm/s have been reported. At regions behind the sills, where water depths are greater than 200 m, generally the velocity is less than 20 - 30 cm/s. This synoptic description of velocity distribution is very useful; it points out areas near the entrance to Glacier Bay where currents are strong and variable, which are ideal locations for future ADCP deployments. Measurements of current velocity in the deep basins, where current velocities are typically at low, are of secondary importance.

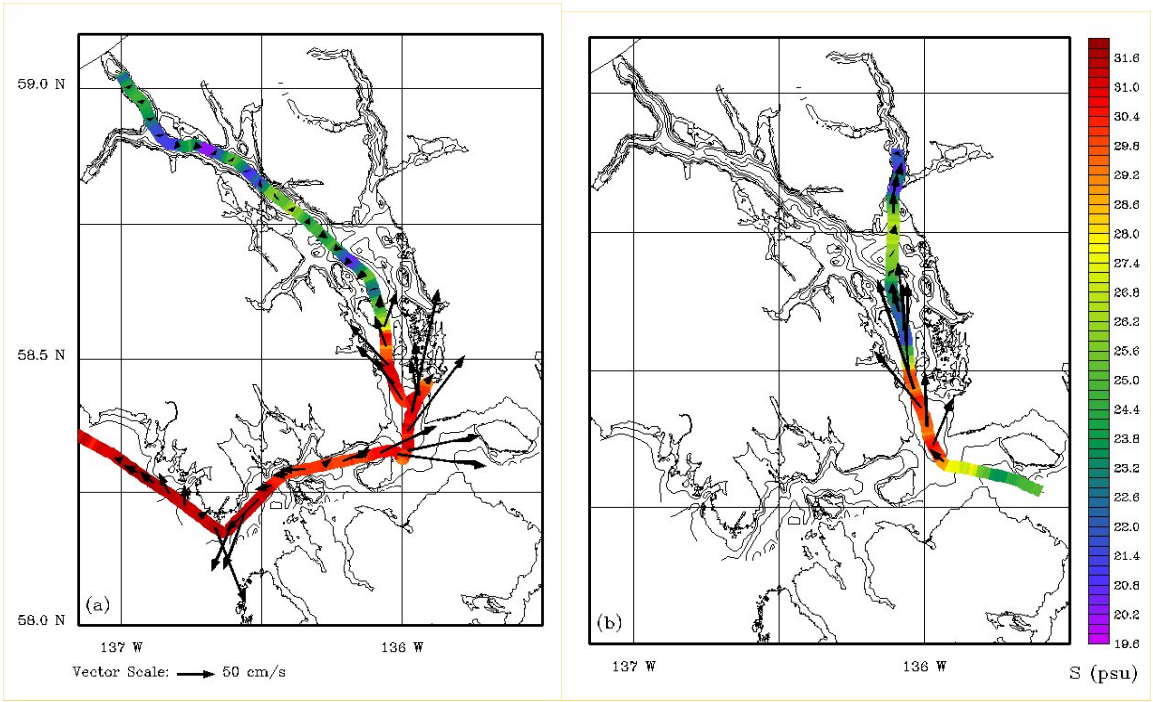

Figure 3. Spatial distribution of tidal velocity measured by a profiling ADCP and CTD measurements on August 8, 2003 (with permission from Cokelet et al., 2006).

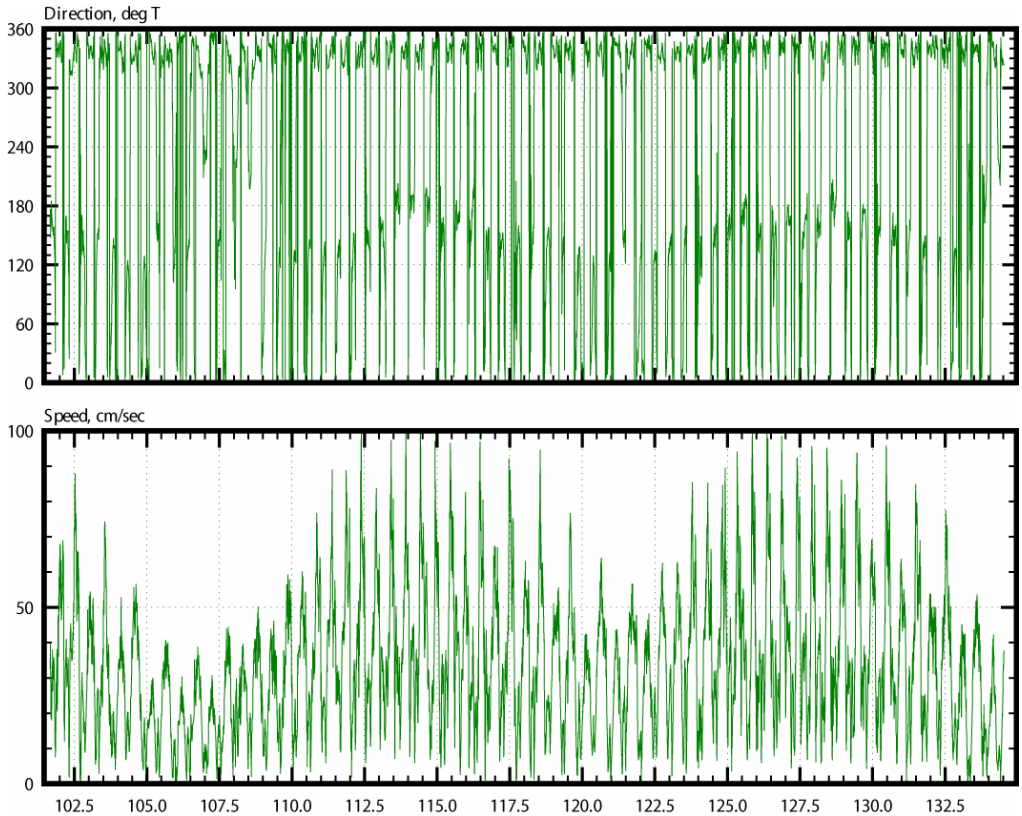

Figure 4. Time-series of tidal current near Bartlett Cove (See location in Figure 2) measured by an electric-magnetic current meter moored at 2.5 m above bed (Kipple, 2006). The horizontal axis is time in calendar days of year 2001.

The only known tidal current time-series was measured by Kipple (2006) between April 11, 2001 and May 14, 2001 at a location near Bartlett Cove where water depth was 56 m at high slack tide

(See S4 in Figure 2). An S4[3] electric-magnetic current meter was deployed over two Spring-Neap tidal cycles. The S4 current meter was moored at 2.5 m above bed and measurements were taken at 10-minute intervals. The measured speed and direction of the tidal current time-series is depicted in Figure 4. In general both the measured speed and direction are quite noisy, which could be perhaps the nature of electric-magnetic current meter measurements. The time-series does reveal the important spring-neap variations of tidal velocity, with speeds of up to 100 cm/s observed at spring and 50 cm/s or less observed during neap. The velocity vectors are noisy and not quite bi-directional. Because this is the only known current measurement, it is difficult to draw any definitive conclusion about the extent of measurement uncertainties. Clearly additional time-series measurements of current (perhaps using an in-situ ADCP) at this and other locations in Glacier Bay are much needed for future research.

As a supplement to these measured data, commercial software "Tides and Currents[3]" was used to reconstruct tides and tidal currents in Glacier Bay for comparison with numerical model results. This software is commonly used to predict tides and currents for navigation; thus the prediction of tides and tidal currents are deemed at least to be qualitatively correct. This software is used to reconstruct historical tides and tidal currents in Glacier Bay for comparison with numerical model results.

3. IMPLEMENTING A NUMERICAL HYDRODYNAMIC MODEL FOR GLACIER BAY, ALASKA

3.1 Important Physical Processes

Many important physical processes are taking place in Glacier Bay, and many important questions remain unanswered. In the false color satellite image shown in Figure 1, the light blue water represents high sediment laden water that originated from melting glaciers and is being transported toward the mouth of Glacier Bay. Tidal velocities near the heads of Glacier Bay are very weak (<20 cm/s); thus vertical mixing is probably not intense. The salinity of the melting water is relatively low and consequently density stratification is likely to form and internal waves could be propagating in these deep basins. Sills, as regions of rapidly changing water depth, are also expected to have strong effects on oceanographic processes. How do the deep bathymetry, sills, and contractions affect the estuarine and fjord circulation, and mixing of the water column? Near sills and constrictions, tidal currents can be as high as 3 m/s and tidal fronts are evident from satellite images. What are the properties of tides that propagate in and out of the system, to what extent are the tides amplified at the heads of the bay, and what are the phase shifts? What are the ranges of tidal currents at the various locations in Glacier Bay? How would the internal waves affect the vertical mixing at the various parts of the bay? Many of these questions can be addressed by means of a numerical hydrodynamic model.

This study is an initial attempt to use a numerical model to answer some of these questions, and to characterize these oceanographic processes. Because time-series data are lacking, the objective of the present effort is limited to developing a Glacier Bay hydrodynamic numerical model to characterize tidal circulation and tidal time-scale processes. Refinements can be introduced to this basic model in the future for the purposes of investigating specific aspects of physical processes in Glacier Bay.

---

[3] Any use of trade, product, or firm name is for descriptive purposes only and does not imply endorsement by the U. S. Geological Survey.

3.2 Modeling Considerations and the Governing Equations

To characterize the hydrodynamics in Glacier Bay, Alaska, a three-dimensional, baroclinic, numerical hydrodynamic model (UnTRIM, Casulli and Zanolli, 2002, 2005) has been implemented to simulate tidal circulation and salinity distribution. Spatial variations of the basin bathymetry play a very important role in circulation properties. The numerical model uses an unstructured grid in the computations that allows an accurate representation of the complex basin topography (Figure 1).

The governing equations for three-dimensional, baroclinic, environmental flows and the transport of conservative scalar variables are the conservation equations of mass and momentum, the conservation equations for solutes, an equation of state, and a kinematic free-surface equation. The fjord/estuarine systems are assumed to be sufficiently large so that Coriolis acceleration is included in the momentum equations. Further, the water is assumed to be incompressible; the pressure is assumed to be hydrostatic, and the Boussinesq approximation applies. In Cartesian coordinates, the governing equations are the continuity equation,

$$Div(\vec{U}) = 0 \quad , \tag{1}$$

the kinematic free-surface equation (integrated continuity equation),

$$\frac{\partial}{\partial t}\eta + \nabla \bullet \left[\int_{-h}^{\eta} \vec{V}\, dz \right] = 0 \quad , \tag{2}$$

where Div ( ) is divergence in three-dimension; $\vec{U}$ is the three-dimensional velocity vector; $\vec{V}$ is the horizontal velocity vector; and $\nabla\bullet(\ )$ denotes the divergence on the horizontal plane. The horizontal momentum equation in an arbitrary direction is,

$$\frac{DV_j}{Dt} - f(\nabla \times \vec{V}) \bullet \vec{N}_j = \frac{\partial}{\partial z}(\nu_v \frac{\partial}{\partial z} V_j) + \nu_h \nabla^2 V_j - g\frac{\partial}{\partial N_j}\frac{\eta}{} - \frac{g}{\rho_o}\frac{\partial}{\partial N_j}\int_z^{\eta}(\rho - \rho_o)dz' \tag{3}$$

where $\vec{N}_j$ is a unit vector on the horizontal plane; $\frac{\partial}{\partial N_j}(\ ) = \vec{N}_j \bullet \nabla(\ )$ is the gradient in $\vec{N}_j$ direction; V_j is the velocity component in $\vec{N}_j$ direction; $\frac{D}{Dt}$ is the substantial derivative; and $\nabla\times(\ )$ is the cross-product on the x-y plane. The transport equation for salt and conservative solutes, C_i, is

$$\frac{D}{Dt} C_i = \frac{\partial}{\partial z}(K_v \frac{\partial}{\partial z} C_i) + K_h \nabla^2 C_i \quad ; \tag{4}$$

and an equation of state relating the water density as a function of salinity and temperature,

$$\rho = \rho_o [1 + \alpha s + \beta(T - T_o)^2] \quad ; \tag{5}$$

where $\alpha = 7.8 \times 10^{-4}$ and $\beta = 7 \times 10^{-6}$, and

(u, v, w) are (x, y, z) velocity components;
η is the free-surface elevation measured from a reference datum;
ρ and ρ_o are density and a reference density;
f is Coriolis parameter;
ν_v and ν_h are vertical and horizontal eddy viscosity;
K_v and K_h are vertical and horizontal eddy diffusivity;
C_i are conservative solutes, i = 1,2,3,…..;

s is salinity in practical salinity units (psu);
T and T_o are temperature and a reference temperature in ^{0}C, respectively.

For three-dimensional barotropic flows (constant density), the solute transport equation is un-coupled from the momentum equations. The governing system of equations, Eq.(1) –Eq.(5), can be solved efficiently by a semi-implicit finite-difference method over a regular computational mesh as discussed by Casulli and Cheng (1992) and Casulli and Cattani (1994). For baroclinic flows, the transport equations are coupled with the momentum equations through the density gradient terms. The baroclinic forcing terms (density gradients) are treated explicitly in the momentum equations, and the solutions of the transport variables are solved lagged one time-step. A user defined turbulence closure is used, and a non-negative bottom friction coefficient is specified to describe the bottom turbulent boundary layer.

3.3 Summary of the Numerical Algorithm for UnTRIM

Traditionally the governing equations are solved over a finite-difference grid. The limitations of a finite-difference grid can be removed by introducing an unstructured computational mesh in which fine grid resolutions are used in complex regions, and relatively coarse grids are used in broad and open areas. This logical extension is possible and still retains the numerical properties of the semi-implicit finite-difference method for solving the shallow water equations (Casulli and Zanolli, 1998; Casulli and Walters, 2000). The numerical algorithm of UnTRIM is fundamentally the same as TRIM3D (Casulli and Cheng, 1992; Casulli and Cattani, 1994), except the finite-difference treatment of the governing partial differential equations is performed over an unstructured grid mesh. The horizontal domain of interest is covered by a set of non-overlapping, convex orthogonal polygons. See a concise definition of an unstructured orthogonal grid in Casulli and Zanolli (1998). The special cases of unstructured orthogonal grids include, of course, the rectangular finite-difference grids, as well as a grid of uniform equilateral triangles. In practice, combinations of three-sided and four-sided polygons are used to represent the domain. The positions of each node, and each polygon, and all connectivities of nodes, sides, and polygons must be defined in the input to the model. The distance between the centers of two adjacent polygons that share a common side must be non-zero. In the vertical dimension, layers of horizontal surfaces divide the domain, and the thickness of the layers can be variable (z-planes). The water surface elevation is defined at the center of the polygon, and assumed to be constant within each polygon. The velocity component normal to each face of a prism is assumed to be constant over the face. The true velocity is defined at each vertex in the middle of each layer. Spatial distribution of velocity is obtained by interpolation, and the water depth of the basin is specified and assumed constant on the sides of polygons.

A semi-implicit finite-difference scheme is applied to obtain an efficient numerical algorithm whose stability is independent from the free-surface gravity wave, wind stress, vertical viscosity and bottom friction. For each polygon, the momentum equation, Eq.(3), is finite-differenced in the direction normal to each vertical faces. The momentum equation relates the gradient of water surface elevation between the centers of adjoining polygons to the face velocity (velocity normal to the face) on the face common to these polygons. The vertical mixing and the bottom friction are discretized implicitly for numerical stability (Casulli and Cheng, 1992; Casulli and Zanolli, 1998). An explicit finite-difference operator is used to account for the contributions from the discretization of the advection and horizontal dispersion terms. A particular form for this operator can be given in several ways, such as by using an Eulerian-Lagrangian scheme (Casulli and Cheng, 1992). For stability, the implicitness factor θ has to be chosen in the range $\frac{1}{2} \le \theta \le 1$ (Casulli and Cattani,

1994). Along the vertical direction, a simple finite-difference is adopted. In general, the vertical thickness of the top and bottom layers can vary depending on the spatial location and the thickness of the top layer can also vary with time. The vertical space increment is allowed to vanish. In fact this is how the wetting and drying of polygons are accomplished.

The free-surface equation, Eq.(2), is discretized implicitly by the θ-method (Casulli and Cattani, 1994; Casulli and Walters, 2000), and only face velocities are needed to complete the volume balance in the polygon (finite volume). By substituting the finite-differenced momentum equations on all faces of a polygon into the continuity equation, the resultant matrix equation governs the water surface elevation distribution for the entire domain (finite-volume method). This matrix equation is strongly diagonally dominant, symmetric and positive definite; thus its unique solution can be efficiently determined by preconditioned conjugate gradient iterations. Once the free-surface for the next time level has been calculated, the normal velocities on the faces of prisms are calculated by back substitution. The details of the finite-difference equations are not reproduced here and readers are referred to Casulli and Zanolli (2002). If baroclinic flows are considered, the transport variables are solved explicitly after the velocity field is solved. The numerical scheme is subject to a weak Courant-Friedrich-Lewy (CFL) stability condition due to the explicit treatment of the baroclinic terms in the momentum equations. It is also subject to a weak stability condition due to the explicit treatment of the horizontal diffusion in the momentum equations.

3.4 Generating an Unstructured Grid for Glacier Bay Hydrodynamic Model

The unstructured computational grid has obvious advantages. It allows the grids to be boundary fitting and allows an arbitrary local grid refinement to meet the needs of resolving fine spatial resolution and placing coarse grids in regions of secondary importance to save computing time. Although methods and literature exist for model grid generation, the process of model grid generation can be quite complicated (Lippert and Sellerhoff, 2006). Some aspects of an unstructured model grid are similar to those used in finite-element applications; therefore the literature in finite-element grid generation might be applicable and useful for UnTRIM model grid generation. The new unstructured grid modeling flexibility is facing new challenges associated with issues of grid generation. In order to take full advantage of these new model flexibilities, the model grid generation should be guided by insights into the physics of the problems, which may require a higher degree of modeling skill.

For the purposes of generating a grid for the UnTRIM model, a commercial product for mesh generation, "Argus"[3], has been adopted. This package is designed for mesh generations in connection with general finite element computations. The output from "Argus" is reformatted to become compatible with the requirements of UnTRIM. Initially a boundary domain file for Glacier Bay is prepared that defines the domain of interest. Within the domain, small islands are excluded, but large islands are included, Figure 5 (left). Then the bathymetry of Glacier Bay (water depth distribution) is introduced, Figure 5 (right). The water depth varies from a few meters up to 400 meters. Sufficiently high resolution in bathymetry data is necessary in order to generate a computational grid mesh that realistically represents the geometrical properties of the bay. Based on these inputs, Argus is ready to generate a triangular or quadrilateral mesh. The user has controls over the grid resolution and grid distribution over the domain to achieve a desirable mesh that

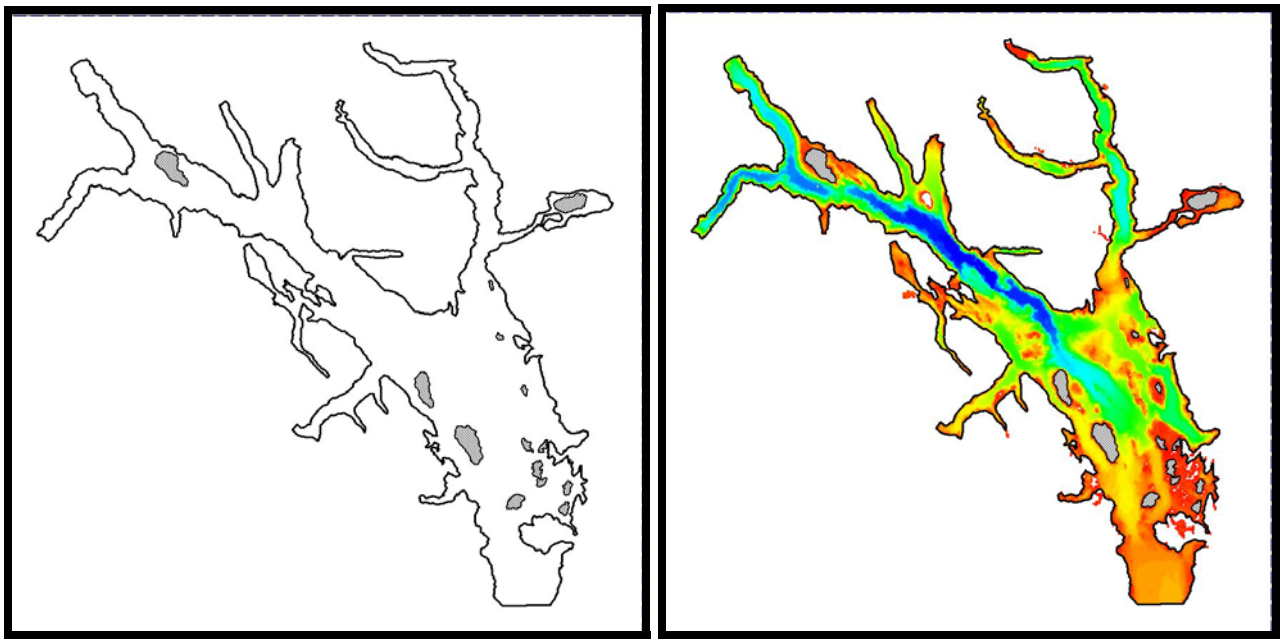

Figure 5. Glacier Bay is defined by a closed contour; large islands (shaded) within the bay are also defined by closed contours inside the domain of interest (left). Bathymetry distribution in Glacier Bay, Alaska where water depth is up to 400 meters in deep basins behind sills of less than 50 meters (right).

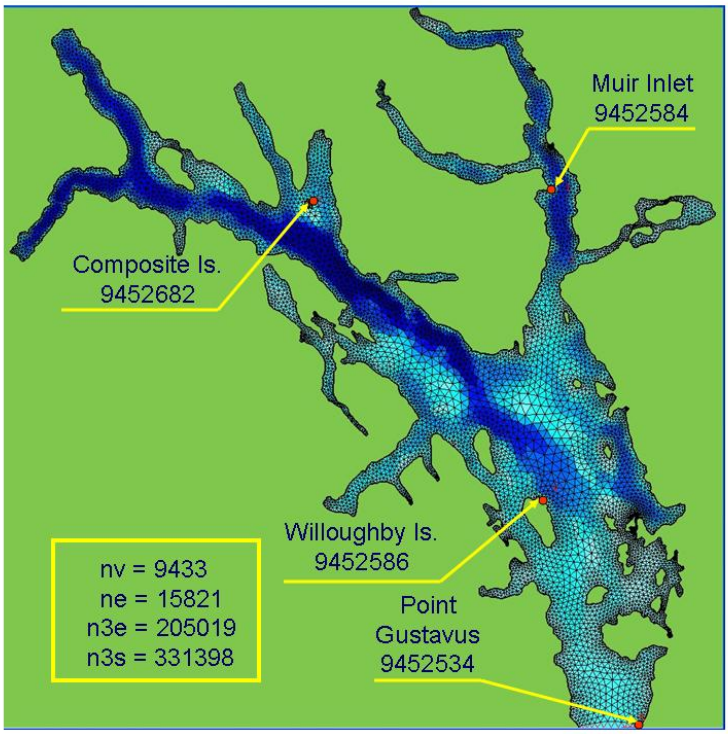

Figure 6. The unstructured grid for Glacier Bay model is shown along with the locations of NOAA tide stations. Properties of the model grid are checked and reported by the UnTRIM model.

captures the salient properties of the basin everywhere. The model grid generated by Argus is not guaranteed to be orthogonal. Another commercial package Janet[3] (Lippert and Sellerhoff, 2006, this conference) is used for grid editing to ascertain that the resulting model grids meet the

requirements of orthogonal unstructured grids. This step might be tedious and requires some experience and skill. However, a computational mesh that properly represents the basin properties is essential in a successful numerical modeling task.

Both the salinity and tidal boundary conditions are specified at the entrance to Glacier Bay. The initial condition assumes that the velocities are initially zero initially, and a spatially distributed salinity from 33 psu at the entrance to 28 psu near the heads representing fresher water from melting glaciers. The UnTRIM model initiates a model run by first checking the properties of the model grid and reports essential model grid properties. The model consists of 15,821 polygons on the horizontal plane and 25 vertical layers resulting in 205,019 3D computational prisms. The sides of the polygon vary from 50 m to 1400 m, Figure 6.

Since the only measured velocity time-series covered the period between April 11 and May 14, 2001, the model simulations are targeted to cover the same time period. Based on the harmonic constants derived for Bartlett Cove (Table 2), a tidal level time series is constructed and imposed at the open boundary where the salinity is assumed to be 33 psu. Based on the estimated propagation of a gravity wave in Glacier Bay, a time-step of a few seconds is required for an explicit numerical model to satisfy the CFL conditions. In this study, the simulation time-step was tested using 60, 120, and 180 seconds, and there were no distinguishable differences in the numerical results or signs of numerical instability. Thus a 3-minute time-step was used to obtain the results discussed in the next section.

4. PRELIMINARY MODELING RESULTS

Due to the paucity of field data (time-series), it is difficult to carry out a rigorous model validation. At this stage, only a confirmation that the numerical model qualitatively represents the hydrodynamic properties in Glacier Bay is sought. Shown in Figures 7 and 8 are the tidal circulation patterns computed by the model at near maximum ebb and maximum flood. The background colors represent either the surface salinity values (Figure 7) or water depth (Figure 8), an important property of the model. These results show that the tidal currents are over 2 m/s between the mouth of the bay and Sitakaday Narrows (entrance sill), and higher velocity is found over the sill at the entrance to Muir Inlet. Otherwise the velocity is generally weak in regions where water is deeper than 150 m and at locations near the head of the bay. These computed velocity patterns can be compared with the ADCP profiling velocity measurements (Figure 3). They agree in identifying the same regions where intensive velocities are found and regions where tidal currents are expected to be weak.

The measured tidal velocity near Bartlett Cove (S4) was compared with the simulated results in Figure 9 over a 30-day period. As the water level varied over spring-neap tidal cycles, the tidal amplitudes varied between 3 to 5 m. The speed of tidal velocity was slightly less than the measured values but their trend was in good agreement. The measured tidal velocity varies from about 30 cm/s during neap to about 70 cm/s during spring. The measured tidal current directions are very noisy and the computed directions are closer to bi-directional; overall the measured and computed values show similar range and behavior.

No other long-term tidal current measurements are available. A tidal current time-series at Sitakaday Narrows was predicted from the “Tides and Currents” software; the predicted time-series is deemed qualitatively correct. The modeled tidal currents were compared with the predicted tidal current time-series at Sitakaday Narrows shown in Figure 10. The tidal range varied between 3.5 m (neap) and over 5 m (spring), and the tidal currents also show strong spring-neap variations with

maximum current speed over 200 cm/s. The tidal current directions are basically bi-directional (160 - 340^{o} North), and phases are in very good agreement. Overall the modeled results are in very good agreement with the predicted values.

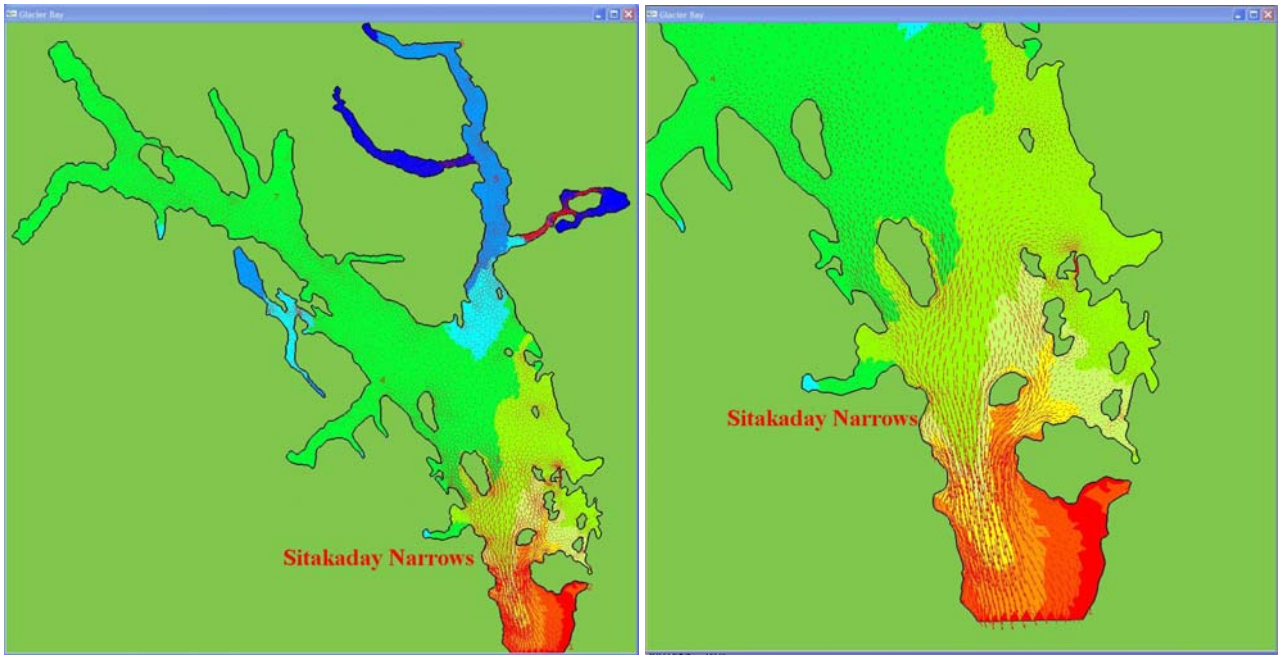

Figure 7. Tidal current distribution near maximum ebb (left) and zoomed in (right) to region near Sitakaday Narrows, where tidal velocity is over 200 cm/s. The background color represents salinity distribution from 33 psu (red) to 28 psu (blue).

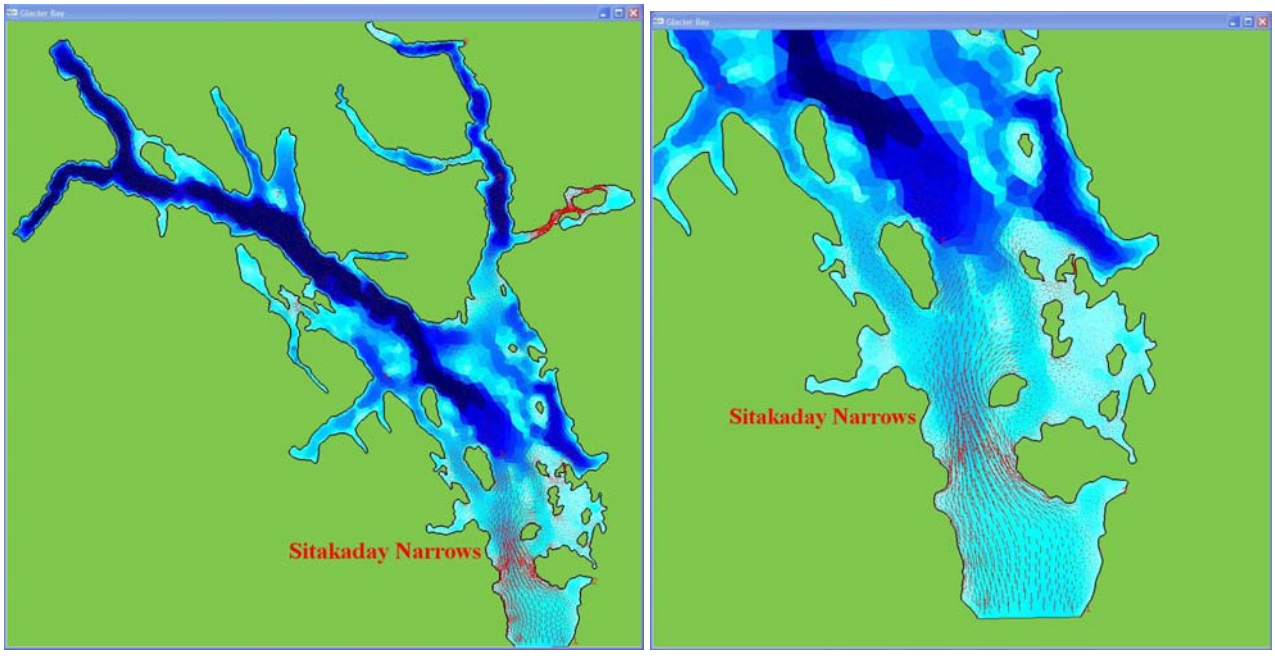

Figure 8. Tidal current distribution near maximum flood (left) and zoomed in (right) to region near Sitakaday Narrows, where tidal velocity is over 200 cm/s. The background color represents water depth distribution from light blue (shallow) to dark blue (over 400 m).

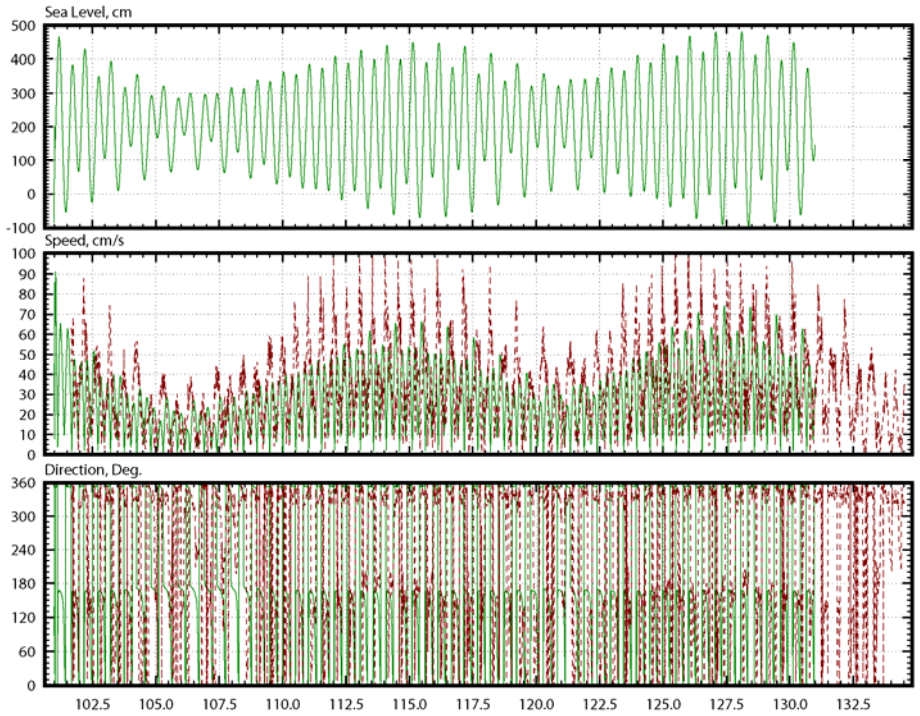

Figure 9. Comparing the numerical model computed time-series (Green) with measurements (Red) made near Bartlett Cove, Alaska (see Figure 2 for location). The horizontal axis is time in calendar days of year 2001.

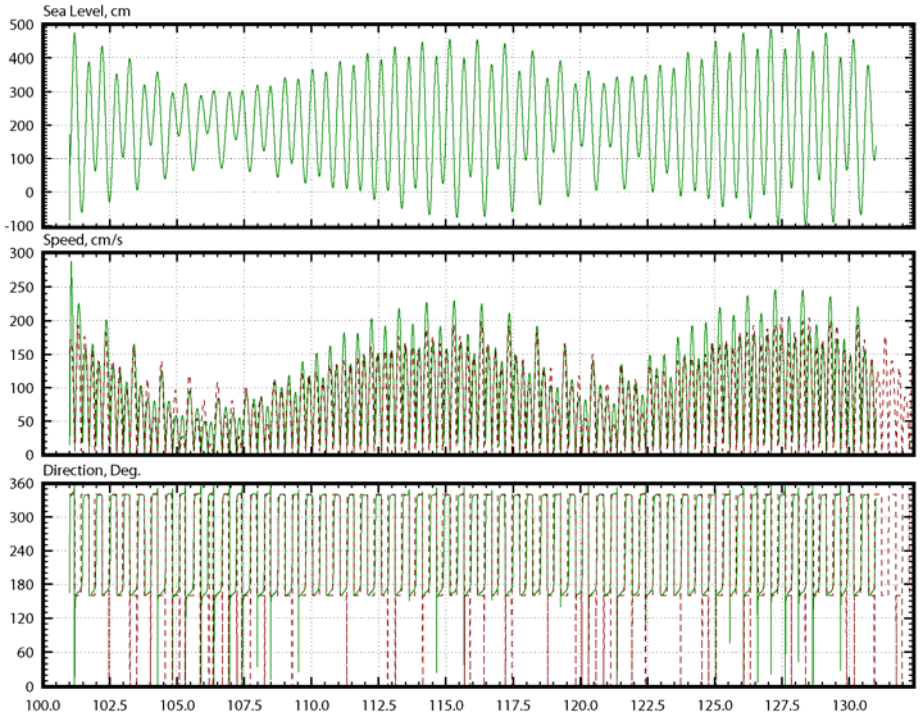

Figure 10. Comparing the numerical model computed time-series (Green) with "Tides and Currents" predicted tidal current at Sitakaday Narrows (Red) (see Figure 2 for location). The horizontal axis is time in calendar days of year 2001.

The simulated tides show about 10% amplification in tidal ranges before the Sitakaday Narrows and up to an hour phase shift. North of Sitakaday Narrows, the tidal range and phase did not show significant changes possibly due to weak tidal currents in the deeper basins.

5. CONCLUDING REMARKS

This study is an initial attempt to use a numerical model to characterize the hydrodynamic properties in Glacier Bay, Alaska. Since the geometry of the bay is quite complex consisting of sills, deep basins and multiple side arms, it is very important for a numerical model to properly represent the salient geometric features of the bay. An unstructured grid numerical model, UnTRIM, has been implemented for this application. There are very limited time-series observations of tides and currents in the bay. The model simulation results, although preliminary, have been shown to be qualitatively representative of the expected spatial circulation patterns as well as the spring-neap cycles of the tides and tidal currents. The simulated tides and tidal currents provide values in the expected ranges. This outcome confirms that this numerical model can be used to understand hydrodynamic characteristics of Glacier Bay and serve as a basic platform upon which to build and guide future research in physical oceanography and hydrodynamics in Glacier Bay. Knowledge of complex oceanographic processes is vital for future interactive interdisciplinary research linking hydrodynamic processes to the distribution and abundance of marine animals in Glacier Bay National Park.

ACKNOWLEDGEMENTS

Permission to reproduce Figure 2 of Cokelet at el, 2006 is acknowledged. David C. Douglas provided satellite images. Blair Kipple, Naval Surface Warfare Center (NSWC), provided S4 current meter data.

REFERENCES

Casulli, V., and Cheng, R. T., 1992, “Semi-Implicit Finite Difference Methods for Three-Dimensional Shallow Water Flow”, Int. Jour. for Numerical Methods in Fluids, 15, 629-648.

Casulli, V., and E. Cattani, 1994, “Stability, Accuracy and Efficiency of a Semi-implicit Method for Three-Dimensional Shallow Water Flow”, Computers & Mathematics with Applications, 27, 99-112.

Casulli, V., and Walters, R. A., 2000, “An Unstructured Grid, Three-dimensional Model Based on the Shallow Water Equations”, Inter. J. for Numerical Methods in Fluids, Vol. 32, p. 331-348.

Casulli, V., and Zanolli, P., 2002, “Semi-implicit Numerical Modeling of Non-hydrostatic Free-surface Flows for Environmental Problems”, Mathematical and Computer Modeling, 36, 1131-1149.

Casulli, V., and Zanolli, P., 2005 “High Resolution Methods for Multidimensional Advection-diffusion Problems in Free-surface Hydrodynamics”, Ocean Modelling, 10, 130-151.

Cokelet, E.D., A.J. Jenkins and L.L. Etherington. 2006, “A Transect of Glacier Bay Ocean Currents Measured by Acoustic Doppler Current Profiler (ADCP)”, Pages XX-XX in J.F. Piatt and S.M. Gende, editors, Proceedings of the Fourth Glacier Bay Science Symposium, 2004. U.S. Geological Survey, Information and Technology Report USGS/BRD/ITR-2006-00XX, Washington, D.C.

Foreman, M. G. G., 1977, “Manual for Tidal Heights Analysis and Prediction, Institute of Ocean Sciences, Patricia Bay, Sidney, B.C., PMS Report 77-10, 66p.

Hooge, P. N., and Hooge, E. R., 2002, “Fjord oceanographic processes in Glacier Bay”, Alaska,

USGS-Alaska Science Center.

Kipple, B., 2006, Personal Communication: Currents measured in Glacier Bay near Bartlett Cove, 2001.

Lippert, C. and Sellerhoff, F., 2006, “Efficient Generation of Unstructured Orthogonal Grids, Proceedings”, Inter. Conf. on Hydroscience and Engineering, September 10-13, 2006, Drexel University, Philadelphia, PA.

Nautical Software, Inc., 1995, Tides and Currents for Windows, Version 2.0a.